Indian Journal of Fibre & Textile Research
Vol. 49, June 2024, pp. 160-172
DOI: 10.56042/ijftr.v49i2.7586

Jute composite based single-leaf structure for sound insulation

M Datta[1,a], B Chatterjee[1], P Ray[2] & D Nath[1]

[1]Department of Textile Technology, Government College of Engineering and Textile Technology, Serampore 712 201, India

[2]Indian Jute Industries Research Association, Kolkata 700 088, India

The present study deals with the development of a mathematical equation that effectively predicts the sound insulation performance of a single-leaf structure constructed using jute composites with varying resin uptake ratios. The investigation employs a reference device to measure the transmission loss (TL) of sound energy as it propagates through a single-leaf structure. The objective is to investigate the impact of structural parameters, namely thickness, theoretical density, and compaction factor, on the attenuation of sound waves within the frequency range of 50–3150 Hz. It has been revealed that an increase in resin uptake, i.e. lower fibre content, is associated with a higher occurrence of voids inside the structure. The presence of voids inside the jute composites is inversely related to TL, while at a given fibre content, transmission loss is linearly related to the areal density of a single-leaf structure, regardless of the thickness of the jute composite. The derived equation for predicting the transmission loss of sound propagating through a single-leaf is expressed as the modified mass law of sound. This equation demonstrates that the mass of an individual leaf structure has a substantial effect on transmission loss, surpassing the influence of frequency. The study provides evidence that the jute composite can be engineered to achieve a degree of transmission loss that is comparable to the materials commonly used for sound insulation applications.

Keywords: Compaction factor, Jute composite, Mass law of sound, Resin transfer moulding, Single-leaf structure, Sound insulation, Transmission loss

1 Introduction

Sound insulation is a crucial component of sustainable development, as it plays a significant role in addressing various concerns, such as public health, urban planning, sustainable consumption, climate change mitigation, and educational environments. Through the mitigation of noise pollution and the promotion of eco-friendly methodologies, sound insulation contributes to the realisation of the United Nations' objective of establishing a fair, robust, and sustainable global community. However, it is worth noting that sound insulation is not explicitly specified within any of the 17 goals, or the 169 associated targets outlined in the Sustainable Development Goals (SDG) framework[1]. Hence, it is imperative to have a comprehensive understanding of the principles of sound insulation to develop appropriate solutions for reframing the SDG.

Based on the mode of transmission, the sound that individuals seek to insulate can be categorised into two types, viz airborne sound, which arises from the oscillation of air particles, and solid-borne sound, which results from impacts on materials or vibrations within solids. The phenomenon of sound permeation adheres to the principles outlined in the 'mass law'[2] within the field of acoustics. The sound insulation efficacy of a wall or plate is contingent upon its mass-to-area ratio[3,4]. The insulating quality of a material improves as its mass increases, resulting in a higher difficulty for vibration to occur. Hence, it is more advantageous to go for materials with high density and weight, namely clay brick, reinforced concrete, and steel plate, for the purpose of sound insulation[5].

In recent times, there has been significant focus on the utilisation of natural fibres in the development of sound-absorbing textiles, especially jute[6–9]. The porous absorber based of fibrous material used for noise suppression has been shown to have a limitation of low transmission loss at lower frequencies[10]. The propensity for fibrous assemblage to undergo shredding throughout its utilisation[11,12] and its inadequate dirt release properties during cleaning and maintenance necessitate the need for a support system, rendering it unsuitable for standalone use[13]. There is a belief that the limitations of fibrous porous absorber can be addressed through the development of composites based on natural fibre[14–17]. The noise control material based on rigid composite possess a

[a]Corresponding author.
E-mail: dattamallika8@gmail.com

high degree of effectiveness in isolating the power of noise (measured in decibels) as compared to its porous fibrous counterpart[18]. The performance of a dense, consistent solid plate for the purpose of reducing undesired acoustic noise and mechanical vibrations within the sonic frequency range is governed by the principle of mass law[2]. Designing an efficient single-leaf structure is crucial for effectively reducing sound at lower frequencies[19]. This is particularly challenging in lightweight and compact solution systems, where sound mitigation becomes more complex. The existing research with the objective on the designing of a single-leaf structure based on jute composite (CJ) for noise mitigation, following the principles of the 'mass law of sound,' is currently restricted[20].

The present study, therefore, involves in the manufacturing of a single-leaf insulator that aimed to decrease noise levels by utilising a combination of jute nonwoven and polyester resin matrix in a composite material. The study also elucidates the necessity to modify the mass law of sound and its application in accurately predicting the sound insulation properties of a single-leaf structure constructed from the jute composite. The novelty of this study lies in its ability to forecast the insulation behaviour of a jute-based single-leaf structure. This is accomplished by incorporating a new structural parameter known as the compaction factor (C_f), together with other parameters, such as thickness (L_T/L), density (ρ_{th}).

2 Materials and Methods

2.1 Materials

The selection of jute nonwoven in making composite was made based on three criteria in sequence of following parameters, viz (i) comparatively high strength, (ii) relative high transmission loss (TL) at 3150 Hz, and (iii) higher productivity in terms of punch density (PD) for each category of nominal areal density[17](300, 500 and 700 g/m^2). The results of breaking load and transmission loss were obtained after characterisation of selected three jute nonwoven samples (N1, N2, N3) and details are given in the Table 1. Resin solution comprising general-purpose polyester resin, catalyst (methyl ethyl ketone peroxide) and accelerator (cobalt nitrate) were then pumped into the mould under pressure displacing the air at the edges, until the mould was filled for making the composite.

2.2 Methods

2.2.1 Preparation of Jute / Polyester Composite (CJ)

The present study employed the Resin Transfer Moulding (RTM) method using the Phoenix series 2012 machine to produce a jute composite based single-leaf structure. The reinforcement utilised in this study was jute nonwovens that was placed within an 800×800 mm² square mould cavity. The operational sequence of the RTM technique is given bellow:

Preform layup → Closing of mould → Resin injection → Curing → De-moulding

The jute nonwoven preform was spread over the female section of the mould of RTM machine. The targeted thickness (L_T) was achieved by varying the number of jute nonwoven layers, which ranged from 1 to 4, the peripheries of the mould were safeguarded by a black rubber enclosure to avert the flow of resin along the sides during the injection process. The male component of the mould was positioned onto the female rest pad (flange) during the matching process, which was filled with a preform (jute nonwoven) before closing the mould. The mould was effectively sealed using fastening bolts and nuts.

The preform was then injected with a resin mixture through injection vents on one side of the mould followed by displacement of air within the preform through overflow vents on the rear side of the mould until the resin came out through the same. The resin was injected through the vent under the pressure of 238 kPa (35 psi). After soaking of the preform inside the fastened mould, the process underwent a curing at ambient temperature over 3-4 h, depending on the target thickness of the final products. The CJ samples were then extracted from the mould. Theoretical fibre weight fractions of 25%, 20%, and 17% were achieved by controlling the resin-to-material ratios at 3:1, 4:1, and 5:1 respectively.

2.2.2 Experimental Plan for Preparation of Jute / Polyester Composite (CJ)

The determination of the desired thickness (L_T, mm) of the jute composite relies on the total

Table 1 — Particulars of selected jute nonwoven for making composite
[Punch density- 19 p/cm^2, delivery speed- 2.5 m/min]

Nonwoven code	Actual areal density g/m^2	Depth of needle penetration of needle loom, mm	Breaking load N (cross / machine direction)	Transmission loss, dB at 3150 Hz
N1	292.2	11	110.87/34.19	2.2
N2	514.2	9	216.3/92.1	3.2
N3	684.5	11	402.15/114.5	3.7

number (n) and thicknesses (t) of the nonwoven jute layers utilised in the development of the final structure. The mass or weight of a composite sample was determined by the areal density (G_A, g/m^2) of the jute nonwoven and the resin to material absorption ratio (R_M). Equation(1) represents the relationship between the theoretical bulk density (ρ_{th}, g/cm^3) of the composite and the variables G_A, R_M, L_T, and n. The stacking thickness of the preform (n×t, mm) was compressed at a pressure of 238 kPa[21]. Here, n denotes the number of jute nonwoven sheets that were positioned on the mould. A composite laminate was manufactured with a target thickness of L_T millimetres. A new parameter, namely the compaction factor (C_f), has been introduced. The mathematical representation of the compaction factor is given by Eqs.(2a) and (2b). The factor includes process factors such as the required thickness of the laminate, the thickness of each individual nonwoven jute layer, and the number of nonwoven jute layers used. Equations (1), (2a), (2b) and (3) are given below:

$$\rho_{th} = \frac{G_A \times (1+R_M) \times n}{10^3 \times L_T} \quad \ldots. (1)$$

$$C_f = \frac{Stacked\ thickness - Target\ Thickness}{Stacked\ thickness}$$

$$= 1 - \frac{L_T}{n \times t} \quad \ldots(2a)$$

$$L_T = n \times t \times (1 - C_f) > 0 \text{ and } C_f < 1 \quad \ldots(2b)$$

$$\rho_{th} = \frac{G_A(1+R_M)}{10^3 \times t\,(1-C_f)} \quad \ldots(3)$$

In theory, it is possible to engineer jute composite based single-leaf structure for sound insulation by varying the constraint applied to produce the structure with a specific target thickness. This can be achieved within a compaction factor range of 0.0-0.7, which is typically attained for composites based on glass fibre at a thickness range 4-12 mm, with a spacing of 4 mm, such was guided by data obtained from widely utilised sound insulation or noise isolation products[22]. The experimentation process involved varying the number of layers (n) between 1 and 4 utilising jute nonwoven samples with specified areal density in each category. Through trial and error, the optimal value for achieving a desired thickness of a CJ sample was determined, with fibre percentages of 17%, 20%, and 25% correspondingly. Despite conducting experiments on all 81 potential sample combinations (3×3^3), it was found that only 27 jute composites could be developed using three jute nonwovens (N1, N2, N3) as per boundary condition given in Eq. (2b) and the specifications of glass fibre composite[22]. Table 2 presents the comprehensive details of the experimental design, encompassing a total of 27 samples, specifically devised for the purpose of manufacturing composites.

2.2.3 Evaluation of Material Characteristics of Jute / Polyester Composite

Jute polyester composite samples were characterised in terms of mass per unit area, thickness, tensile strength, flexural strength, impact strength, and transmission loss. The samples were subjected to conditioning in 20±2°C and 65±2% relative humidity for 48 h prior to each test. The actual thickness (L) of the composite in mm was measured with a digital slide calliper having an accuracy of 0.01 mm. The Orpat India electronic balance was used to measure the sample weight in kg of each 300×300 mm^2 sample. Based on this weight, the mass per unit area of the composite sample in kg/m^2 was calculated. For the tensile, flexural, and impact tests, the standards employed were ASTM D683-86, ASTM D 790-71, and ASTM D 256-10 respectively. The universal testing machine (FIE Universal Testing Machine, Model Number: Ute-10, India) was employed for tensile and flexural strength testing, while the pendulum impact tester (XJJ-50, China) was used for impact strength testing. The tests were conducted 10 times for each resin-to-jute ratio to ensure reproducibility. The actual bulk density (ρ_A) of each sample was calculated in g/cm^3 based on its measured weight and thickness. Void content of the composite was determined based on actual bulk density (ρ_A) and theoretical bulk density (ρ_{th})[23], using the following equation:

$$V(\%) = \frac{\rho_{th} - \rho_A}{\rho_{th}} \times 100 \quad \ldots (4)$$

2.2.4 Transmission Loss (TL)

In this research, a device[24] (Fig. 1) was designed to assess the noise control properties of jute composite material within the frequency range of 50-3150 Hz, specifically in the 1/3-octave band. The designed device quantifies transmission loss (TL). The device comprises six main elements, namely a function signal generator, a variable signal amplifier, a sound source (a loudspeaker), a sound chamber, a sound detector [the probe of a digital sound meter that displaying sound power in decibels (dB)], and a material sample holder. The instrument was calibrated using a standard glass pane of 6 mm thickness[22]. This

Table 2 — Experimental design for making composite laminate

Resin to material uptake ratio (R_M)	Areal density of jute nonwoven g/m^2 (CV%)	Thickness (t) of nonwoven jute layer, mm(CV%)	Target thickness of composite (L_T), mm	Number of nonwoven jute layer (n)	Final thickness of CJ composite (L), mm (CV%)	Compaction factor (C_f)
3:1	292.2 (17.8)	3.03 (13.4)	4	2	4.9 (2.1)	0.1914
			8	3	8 (1.9)	0.1199
			12	4	11.4 (1.5)	0.0594
	514.2 (13.7)	4.44 (12.1)	4	1	4.0 (2.0)	0.0991
			8	2	8.1(1.9)	0.0878
			12	3	12.0(2.5)	0.0991
	684.5 (12.9)	5.36 (11.2)	4	1	4.3(3.2)	0.1978
			8	2	9.2(2.1)	0.1418
			12	3	14.0(2.5)	0.1294
4:1	292.2 (17.8)	3.03 (13.4)	4	2	4.9 (3.2)	0.1914
			8	3	8.0 (2.6)	0.1199
			12	4	11.2 (3.2)	0.0759
	514.2 (13.7)	4.44 (12.1)	4	1	4.0(2.1)	0.0991
			8	2	8.1(2.5)	0.0878
			12	3	12.2(1.9)	0.0841
	684.5 (12.9)	5.36 (11.2)	4	1	4.5(2.7)	0.1604
			8	2	9.5(3.6)	0.1138
			12	3	14.2(4.1)	0.1169
5:1	292.2 (17.8)	3.03 (13.4)	4	2	5.0 (3.9)	0.1749
			8	3	8.0(2.6)	0.1199
			12	4	11.2(2.9)	0.0759
	514.2 (13.7)	4.44 (12.1)	4	1	4.0(3.3)	0.0991
			8	2	8.5(4.1)	0.0653
			12	3	12.3(3.2)	0.0766
	684.5 (12.9)	5.36 (11.2)	4	1	4.6(3.5)	0.1418
			8	2	9.4(3.9)	0.1231
			12	3	14.2(4.5)	0.1169

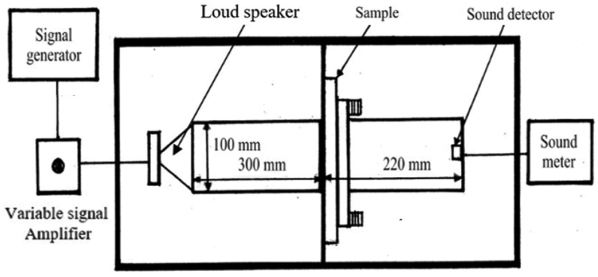

Fig. 1 — Schematic diagram of developed device for measuring transmission loss

glass sheet, commonly used in building construction as a noise control glass pane, has a transmission loss of 36 dB at a frequency of 4000 Hz. The transmission loss (TL) was calculated using the decibel (dB) values obtained from the digital sound meter in two scenarios, viz without a sample present (D_{wos}) and with a sample present (D_{ws}) in front of it, using the following equation:

$$TL = D_{wos} - D_{ws} \quad \ldots (5)$$

2.2.5 SEM Study

The specimens were promptly affixed to aluminium SEM stubs using a two-sided adhesive sheet and subsequently covered with a thin carbon coating employing HHV BT300 (Hind High Vacuum Company Pvt. Ltd., India). The surface morphology of the samples was analysed using the ZEISS EVO 40 SEM (Carl Zeiss AG, England), which yielded comprehensive insights into the fractured surface and voids present in the composites under 15.0 kV.

3 Results and Discussion

3.1 Bulk Density and Void Content of Jute Polyester Composite (CJ)

The percentage of void content in the CJ sample is determined by the Eq. (4), which involves the utilisation of actual and theoretical bulk density data as presented in Table 3. Fig. 2 illustrates the influence

Table 3 — Structural parameter and transmission loss of jute polyester composite

Sample code	Fibre content, wt %	Resin-material uptake ratio (R_M)	Actual bulk density kg/m^3	Theoretical bulk density kg/m^3	Void %	Actual areal density kg/m^2	Final thickness of CJ composite (L), mm (CV%)	Compaction factor (C_f)	Tensile strength MPa	Flexural strength MPa	Impact Strength kg.m	Transmission loss in dB (at central frequency of seven 1/3- octave bands)						
												50 Hz	100 Hz	200 Hz	400 Hz	800 Hz	1600 Hz	3150 Hz
CJ1	25	3:1	432.00	476.73	9.38	2.12	4.9 (2.1)	0.1914	45.50	63.87	0.04	13	16	18	22	23	25	31
CJ2			406.88	438.00	7.10	3.26	8 (1.9)	0.1199	42.76	63.58	0.04	19	22	24	28	29	31	38
CJ3			384.56	409.82	6.16	4.38	11.4 (1.5)	0.0594	41.53	59.42	0.04	23	26	28	32	33	35	43
CJ4			461.99	514.00	10.11	1.85	4.0 (2.0)	0.0991	60.29	76.37	0.06	12	15	17	21	22	24	32
CJ5			460.00	507.65	9.39	3.73	8.1(1.9)	0.0878	60.52	68.64	0.05	21	24	26	30	31	33	40
CJ6			484.44	514.00	5.75	5.81	12.0(2.5)	0.0991	65.33	76.98	0.07	27	32	34	38	39	41	46
CJ7			584.24	636.28	8.18	2.51	4.3(3.2)	0.1978	148.00	87.12	0.11	14	17	19	23	24	26	33
CJ8			559.30	594.78	5.97	5.15	9.2(2.1)	0.1418	145.53	86.54	0.08	26	29	31	35	36	38	45
CJ9			552.42	586.29	5.78	7.73	14.0(2.5)	0.1294	143.58	80.75	0.07	34	36	39	40	42	45	47
CJ10	20	4:1	510.31	595.92	14.37	2.50	4.9 (3.2)	0.1914	33.13	52.4	0.04	17	22	24	27	29	31	38
CJ11			470.45	547.50	14.07	3.76	8.0 (2.6)	0.1199	29.24	49.87	0.03	22	25	27	30	32	34	41
CJ12			463.40	521.43	11.13	5.19	11.2 (3.2)	0.0759	25.03	49.45	0.02	28	30	33	35	38	40	43
CJ13			532.10	642.50	17.18	2.13	4.0(2.1)	0.0991	34.30	50.36	0.05	15	20	22	26	27	29	35
CJ14			558.15	634.57	12.04	4.52	8.1(2.5)	0.0878	55.91	53.49	0.06	26	30	33	37	40	42	42
CJ15			572.00	631.97	9.49	6.98	12.2(1.9)	0.0841	56.86	53.65	0.07	31	34	37	39	41	43	45
CJ16			653.54	760.00	14.01	2.94	4.5(2.7)	0.1604	135.02	63.12	0.08	18	21	25	30	33	35	42
CJ17			650.50	720.00	9.65	6.18	9.5(3.6)	0.1138	113.68	62.45	0.08	30	33	35	38	40	42	44
CJ18			640.00	722.54	11.43	9.09	14.2(4.1)	0.1169	66.00	56.21	0.06	33	37	41	45	47	49	52
CJ19	17	5:1	563.46	700.80	19.60	2.82	5.0 (3.9)	0.1749	37.27	47.26	0.03	26	29	31	33	34	35	42
CJ20			545.00	657.00	17.05	4.36	8.0(2.6)	0.1199	32.67	45.37	0.02	27	30	32	36	37	39	46
CJ21			520.00	625.71	16.90	5.82	11.2(2.9)	0.0759	31.33	42.25	0.02	31	35	39	41	43	47	50
CJ22			619.50	771.00	19.65	2.48	4.0(3.3)	0.0991	46.91	50.97	0.04	18	21	25	30	33	35	41
CJ23			622.32	743.13	16.26	5.17	8.5(4.1)	0.0653	38.73	48.54	0.03	29	32	34	38	39	41	48
CJ24			645.09	752.20	14.24	7.93	12.3(3.2)	0.0766	45.33	49.36	0.03	36	39	41	42	45	49	50
CJ25			721.00	892.17	19.19	3.32	4.6(3.5)	0.1418	66.90	51.2	0.03	28	31	33	38	40	42	46
CJ26			726.00	873.19	16.86	6.82	9.4(3.9)	0.1231	68.60	52.12	0.04	35	38	40	44	45	47	50
CJ27			741.00	867.04	14.54	10.52	14.2(4.5)	0.1169	77.22	55.6	0.05	44	45	49	50	52	53	60

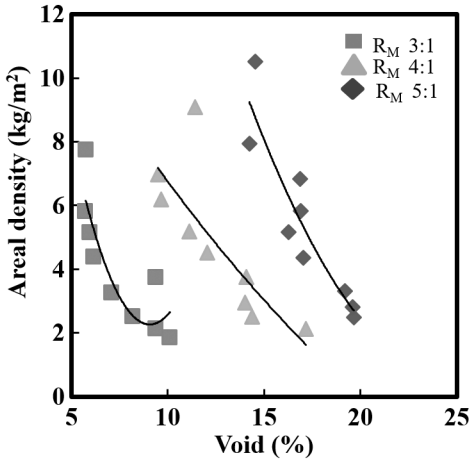

Fig. 2 — Variation in areal density with void (%) at three different resin uptake (R_M)

of void on the areal density of the CJ composites upon varying resin-to-reinforcement ratios (resin uptake, R_M 3:1, 4:1, and 5:1). The presence of voids (encircled by dotted lines) has a discernible impact on the weight of the composite samples, resulting in a reduction in their areal density. This observation holds true across all three resin uptake ratios (R_M). The second-order polynomial regression model produces R^2 values of 0.78, 0.69, and 0.84 for R_M 3:1, 4:1, and 5:1 respectively, which correspond to fibre content percentages of 25%, 20%, and 17%. Typically, the proportion of voids tends to grow as the R_M value increases, which suggests a decrease in the amount of fibre present and an increase in the non-uniformity of the CJ structure. A similar phenomenon is also observed by Hamidi *et al.*[25] in their study on RTM moulded E-Glass/Epoxy composites. They interpreted this occurrence as an evidence of relatively uniform dispersion of reinforcing fibres within the matrix at lower resin content. It is also noted that a lower bulk density corresponds to a lower resin-to-matrix ratio. A void or micro cracks are observed in the scanning electron microscopy (SEM) images of sample CJ9, 14 and 27 (Fig. 3). The micrograph provides visual evidence supporting the hypothesis of higher theoretical density (ρ_{th}) as compared to actual (ρ_A) and higher resin uptake was related higher void content. This can also be inferred from the measured actual bulk density (ρ_A) and theoretical bulk density (ρ_{th}) of the 27 samples (Table 3).

3.2 Mechanical Behaviour of Jute / Polyester Composite (CJ)

The mechanical properties for jute nonwoven polyester composites prepared by RTM process are given in Table 3. The manufacturing of CJ samples involves systematic variation in the parameters, namely resin-material uptake ratio (R_M), thickness (t)

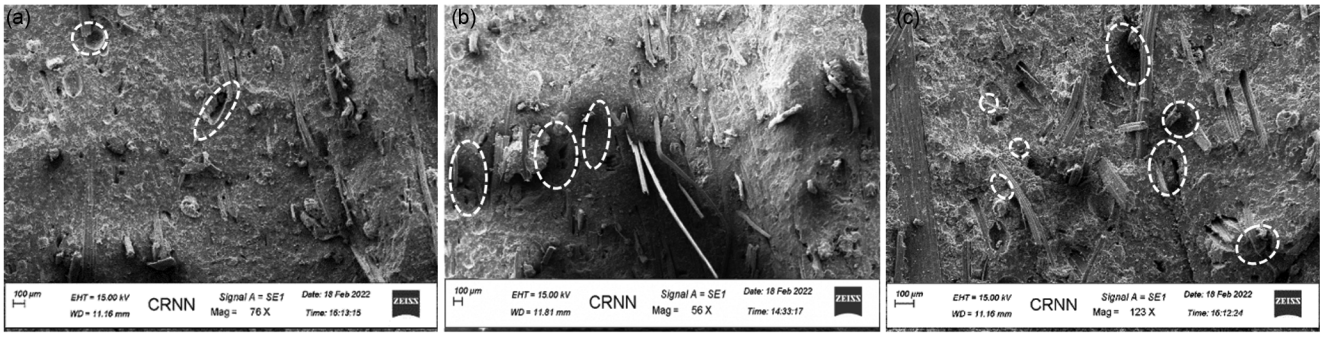

Fig. 3 — Scanning electron microscopic images of voids or micro-crack present in the CJ composite (a) CJ 9, (b) CJ14, and (c) CJ27.

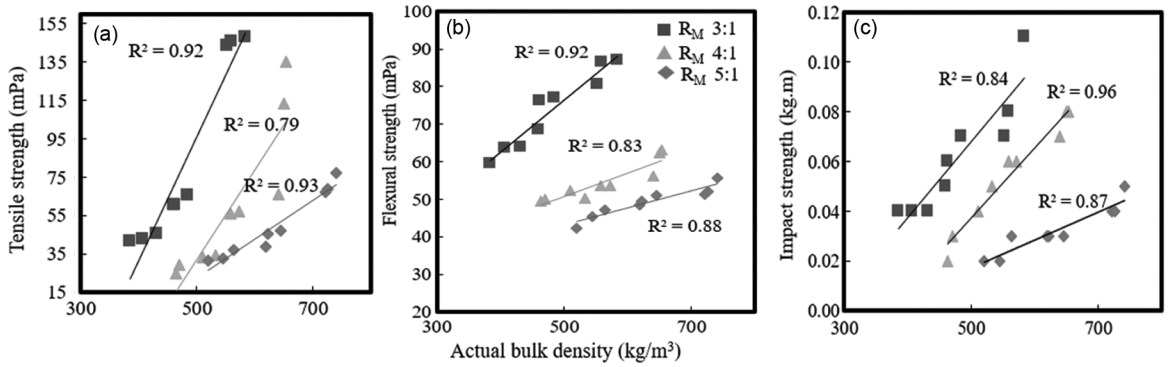

Fig. 4 — Variation of (a) tensile strength, (b) flexural strength, and (c) impact strength with bulk density of CJ composites at three different resin-jute nonwoven uptake (RM 3:1, RM 4:1 and RM 5:1).

of jute nonwoven, target thickness (L_T), and areal density of jute nonwoven (G_A). All these parameters control the amount of fibre and resin in a given volume of CJ, which, in turn, affect the bulk density of the final composite [Eqs.(1) & (3)]. So, attempt has been made to explain the behaviour of the mechanical properties of CJ with the variation of bulk density.

3.2.1 Effect of Bulk Density on Tensile, Flexural, and Impact Strength

The tensile, flexural, and impact strengths of all 27 composite samples are plotted as functions of bulk density, as depicted in Figs. 4(a)-(c), respectively. This presentation aims to elucidate the influence of bulk density on the tensile, flexural, and impact behavior of the developed jute composite-based single-leaf structure.

Figure 4(a) reveals a notable association between the tensile strength (MPa) of the composite structure and its bulk density, when considering a specific R_M i.e. the fibre content. The observed augmentation in strength can be accredited to the phenomena of stress distribution predominantly among the fibres inside the structure, leading to an improved capacity to resist slippage. The observation is also reported by Faradusay *et al.*[26]. On the other hand, with the rise of R_M (reduction in fibre content), the strength of CJ samples drops. The discovery aligns with the presence of voids in the composite structure (Fig. 3) leading to uneven stress concentration during the tensile loading of the same. The observed increase (54.9%) in tensile strength can be attributed to the rise in fibre content from 17% to 25%.

Figures 5(a) and (b) illustrate the scanning electron microscopic images of CJ9 (R_M: 3:1) before and after the onset of tensile fracture. The behaviour of the CJ under tensile stress until it reached its ultimate strength, leading to failure, is illustrated in Fig. 5(b) by tracing out the broken edges of fibres. Fracture in the composite is governed by failure in the reinforcing jute nonwoven other than the failure of matrix. The microscopic image also illustrates that the fractured fibre has experienced a state of disorder after its rupture and pulled up fibre from structure at time of break. The observed phenomena can also be attributed to the existence of voids inside the composite material (Fig. 3).

The flexural strength of all 27 composite samples is illustrated in Fig. 4(b). The correlation between flexural strength and bulk density is found to be positive, as seen by the R^2 values ranging from 0.83 to

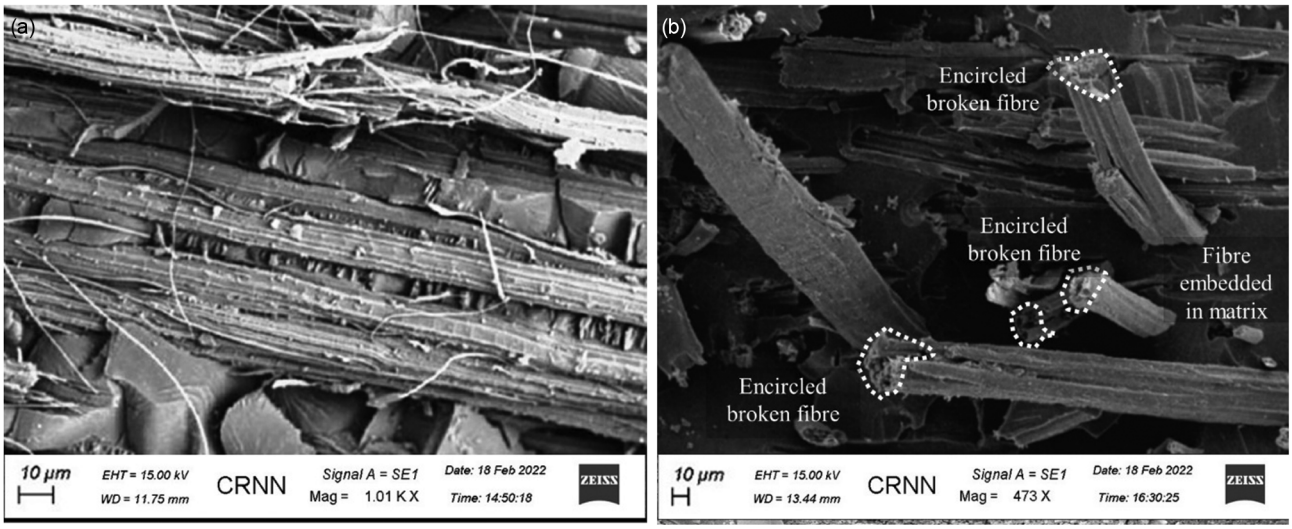

Fig. 5 — Scanning electron microscopic image of composite CJ9 (a) before and (b) after the tensile fracture

0.92. This relationship is valid under the condition that the resin absorption or fibre content, remains constant. The composite material, manufactured by the resin transfer moulding technique, demonstrates a maximum flexural strength of 87.12 MPa at a fibre content of 25%. The flexural strength of CJ8 shows a significant increase of 41.2% when the fibre content is changed from 17% to 25% (R_M: 3-5) The correlation between flexural strength and bulk density across several R_M demonstrated a similar trend to that observed in case of tensile failure. The observed changes can also be ascribed to the same phenomenon as observed in the tensile loading. The cross-sectional shape of the specimen remains same across various R_M during the testing of flexural strength. The flexural strength, which is an inherent characteristic, is influenced by the tensile behaviour when considering its relationship with bulk density[27].

Composite fracture toughness, alternatively referred to as impact strength, pertains to the inherent ability of a material to resist fracture under the influence of rapidly applied force. The parameter of interfacial strength[28] has an impact on it. The impact strength variation of the CJ composites in proportion to bulk density at three varied levels of R_M (fibre content) is depicted in Fig.4(c). The relationship between the impact strength of a CJ composites and the increase in bulk density is found to be linear at given R_M (fibre content). The mass of fibres played a crucial role in augmenting the impact resistance of the composites and serve as a conduit for stress transfer[29]. The impact strength demonstrates a comparable trend to the previously examined tensile and flexural strength. The increase in fibre content from 17% to 25% results in a significant (72.7%) enhancement in impact strength. The data present in the study demonstrates a notable correlation between increased bulk density and enhanced impact strength, particularly when compared to the tensile and flexural strengths of the CJ samples. The increase of impact resistance in relation to bulk density (mass) corroborates the theory of mass control phenomenon of sound insulation of a barrier[30].

3.3 Acoustical Behaviour of the Jute Polyester Composite (CJ)

The areal density of the barrier made of CJ composites is determined by two key elements, namely the fibre content and the resin uptake ratio (R_M). Table 3 displays the structural parameters and transmission loss data for the 27 CJ across central frequencies within the seven 1/3-octave bands ranging from 50 to 3150 Hz. It is found that facilitation of sound energy transfer is achieved through the oscillatory movement of a physical barrier[31,32]. The sound insulation is correlated with frequency, and it corresponds to the mass law[32]. The change of the areal density of the CJ structures at R_M 3:1, 4:1, and 5:1 had an impact on the transmission loss as illustrated in Fig. 6. The increase in transmission loss is directly proportional to the areal density for a given R_M. The findings indicate that there is a correlation between the areal density of CJ and the transmission loss. Specifically, when the areal density is changed from 2.12 to 10.52 kg/m^2, the transmission loss varied from 31 dB for CJ1 to 60 dB for CJ27 at a frequency of 3150 Hz. This

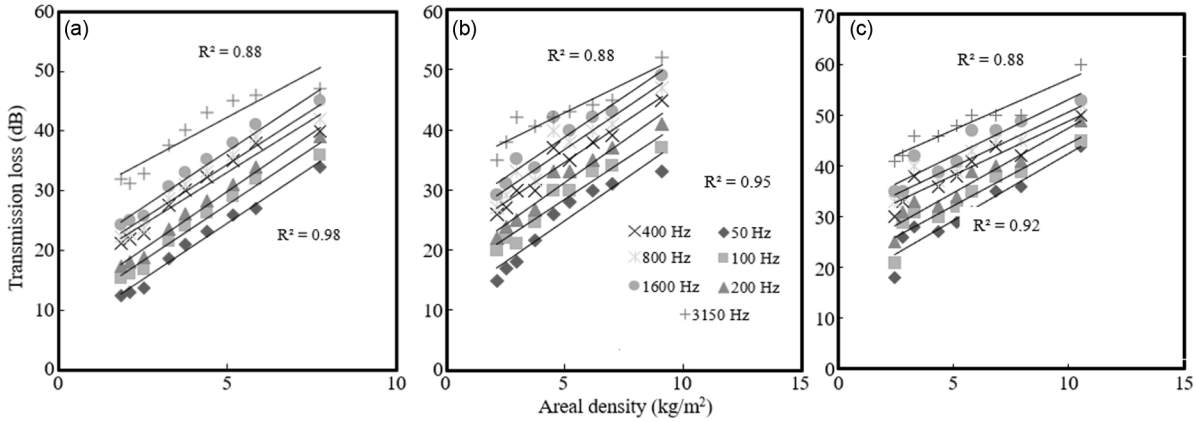

Fig. 6 — Variation in transmission loss of CJ composite with areal density for (a) R_M 3:1, (b) R_M 4:1, and (c) R_M 5:1

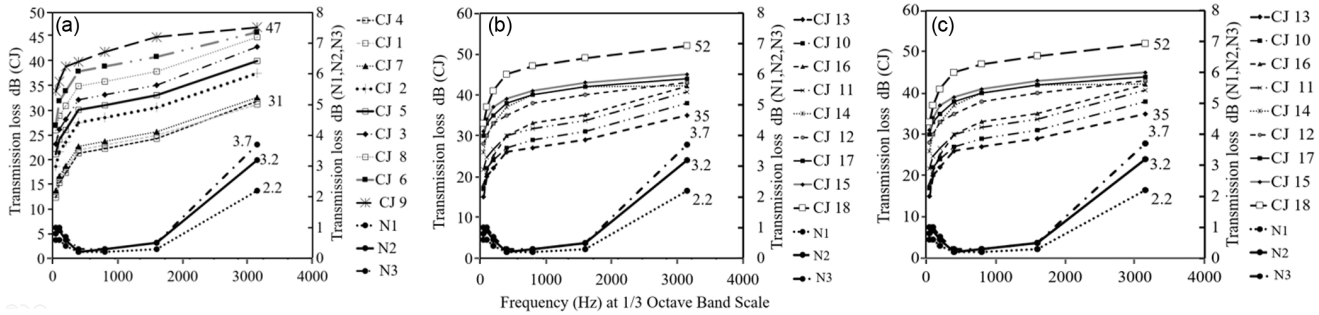

Fig. 7 — Variation of transmission loss of CJ composite with frequency (a) R_M 3:1, (b) R_M 4:1, and (c) R_M 5:1

relationship held true regardless of any changes in thickness (Tables 2 and 3). A substantial favourable association is found between transmission loss and areal density, as evidenced by the R^2 values ranging from 0.88 to 0.98 at R_M 3, 0.88 to 0.95 at R_M 4, and 0.88 to 0.92 at R_M 5. During the propagation through a structure, the incident sound energy induces oscillations inside the mass of this structure which results in the isolation of sound energy by the force of inertia exerted by the mass[32]. The resistance of CJ single-leaf structure is the upshot of flexural vibration that is found to be changed with the changes in ambient sound pressures (dB).

3.4 Effect of Frequency on Transmission Loss

The frequency-dependent transmission loss data for all samples at three different resin uptakes (R_M) are illustrated in Fig.7. It is observed that the transmission loss shows a positive correlation with frequency at a given areal density. The wavelength of the incident sound energy ranges from 6.8 m (50 Hz) to 0.11 m at 3150 Hz. The power of the incident energy to vibrate incident surface with a wavelength of 0.11 m is relatively low[33]. Consequently, a higher dissipation of sound energy is observed at higher frequencies. To facilitate comparison, reinforcing jute nonwovens (N1, N2, N3)are tested for the transmission loss (TL) and plotted alongside the CJ samples. The data shown in the figures indicate a noticeable increase in TL property after the transformation of jute nonwoven into CJ samples.

The transmission loss for all 189 data (27 samples × 7 frequency levels) plotted as a function of the logarithm of the product of areal density (m) and frequency (f) is shown in Fig. 8 (a). The figure shows the relationship with an R^2 value of 0.65 at all central frequencies of the seven 1/3-octave bands (50, 100, 200, 400, 800, 1600, and 3150 Hz). The influence of product of areal density (m) in g/m^2 and frequency (f) in Hz on transmission loss in dB can be represented by the regression model obtained by fitting all these data using MATLAB R2016a, as shown below:

$$\text{Transmission loss} = 11.84 \log(\text{m} \times \text{f}) - 4.44 \quad \ldots(6)$$

The expression for transmission loss in Eq. (6) is influenced by the mass law or frequency law established by Cremer[19]. The predicted TL from Eq. (6) is plotted as a function of the measured TL shown in Fig. 8(b), yielding an R^2 value of 0.59. Model validation is tested using the 'Chi Square' goodness-of-fit distribution[34] over 189 data points with a degree of freedom (df) of 188. The calculated χ^2 value at df

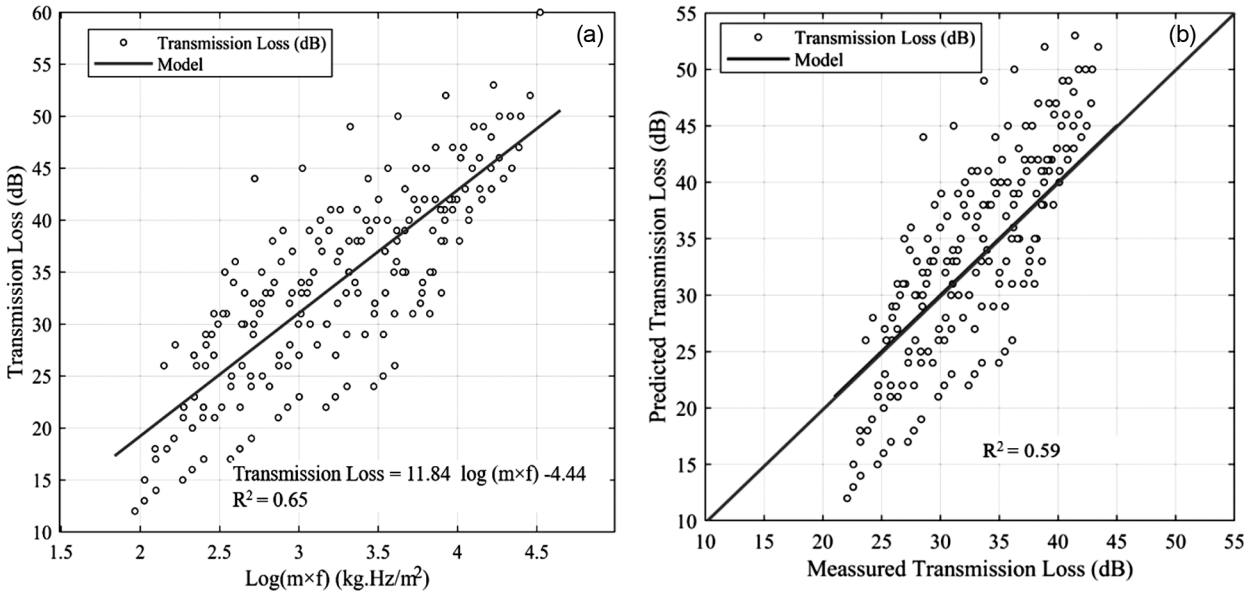

Fig. 8 — (a) Influence of m×f on transmission loss and (b) relationship between predicted and measured transmission loss following Eq. (6)

188 is 204.1, against the tabulated value of 145.85 at the 1% significance level, and the null hypothesis of no difference is rejected. The general mass law expression of sound indicates that the transmission loss is proportional to logarithm of the product of areal density (m) and frequency (f) with same coefficient value. Eq. (6), based on this generic form of the mass law, needs further modification to fit the experimental data of CJ, as the regression equation explained only 59% of the dataset [R^2=0.59, Fig. 8(b)]. Therefore, a basic postulation should be introduced to describe the influence of frequency in Hz and mass (areal density) in g/m^2 on transmission loss in dB with different coefficients. A new model has been developed by best fitting the measured values of TL for a set of 189 data points (Table 3). The least square method[34]is adopted to find the best-fit line, and the generalized expression is as follows:

Transmission loss (TL)=
$33.14\times\log_{10}(m)+9.34\times\log_{10}(f)-11.42$ … (7)

Equation (7) suggests that the impact of mass on transmission loss is more significant than the influence of frequency. Fig. 9 (a) illustrates a 3D surface plot of transmission loss in relation to frequency and actual areal density, serving as the primary factors for prediction over a dataset of 189 points with an R^2 value of 0.90. The degree of scatter in the predicted TL data is found to be reduced when calculated based on [Eq. (7) and Fig. 9 (b)]. This improvement is reflected in the change of the R^2 value from 0.59 to 0.90.

The deviation of predicted value [Eq.(7)] from the experimental one is estimated by the 'Chi Square' goodness of fit distribution over 189 data with a degree of freedom (df) of 188. The null hypothesis is that "there is no difference between experimental and predicted values". The calculated χ^2value at df 188 is 51.22 against the tabulated value of 145.85 at 99.0% confidence level. It implies that there is less than 1% chance of error and the null hypothesis of no difference is accepted. Equation (7) has been modified by replacing m (areal density) of the CJ composite in kg/m^{2}with compaction factor C_f, bulk density ρ_{th}, number of jute nonwoven layer n and thickness of jute nonwoven layer t. The newly developed prediction model can be expressed by the following equation:

$$TL = 33.14\times\log_{10}\{\rho_{th}(1-C_f)n\times t\} + 9.34\times\log_{10}(f) - 11.42 \quad \ldots (8)$$

The expression reveals that the transmission loss of all possible jute composite over the span of R_M of 3:1, 4:1, 5:1 can be predicted with engineering of the structural parameters (L_T, ρ_{th}, C_f) of composite material over frequency range 50- 3150 Hz.

3.5 Effect of Void on Transmission Loss

The presence of void is identified from the scanning electron micrograph of CJ9, CJ14, and CJ27 (Fig.3). The influence of void on transmission loss is presented in Fig.10. The presence of void reduces the

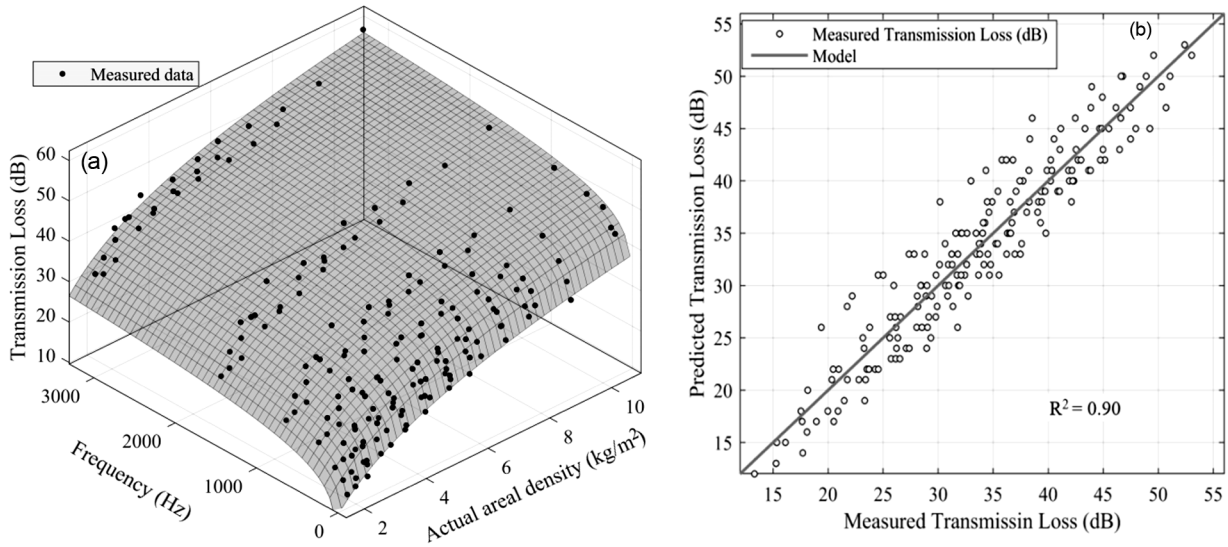

Fig. 9 — (a) Surface plot of transmission loss, and (b) relationship between predicted and measured transmission loss following Eq.(7)

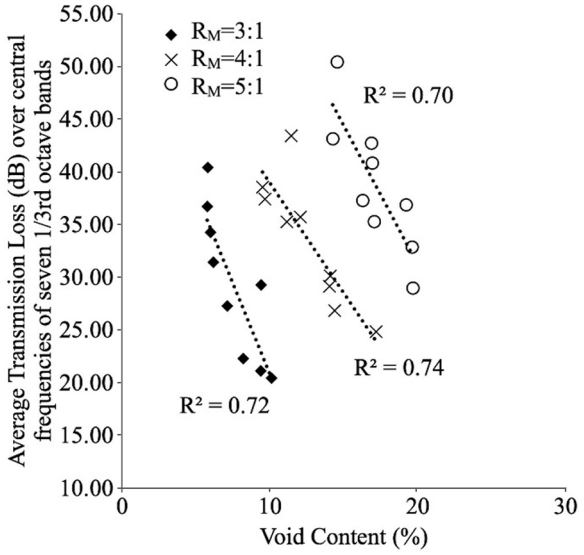

Fig. 10 — Variation of average transmission loss with void (%)

insulation performance in terms of transmission loss as observed from the figure for all three resin take up ratios. Air present in the void, acting as the resistive element given by $\rho_0 c_0$ [ρ_0=density of air, c_0=speed of sound], offers hindrance in the direction of propagation of sound, while the resistance offered by solid mass is equivalent to $m\omega$ [m=mass (areal density),$\omega = 2\pi f$ with f=frequency]. The impact of mass in blocking the sound is more profound for a barrier material[22], as $(m\omega)^2 >> (2\rho_0 c_0)^2$. Moreover, a higher degree of void associated with a lower 'm' facilitates the propagation of sound through the structure due to the presence of heterogeneity within it. The bonding between the reinforcing jutefibres and the matrix material is found as critical as the voids, especially located at the fibre-matrix interface, leading to easy pathway forsound transmission. Void distribution creates "weak spots" of sound transmission, making the material less effective at blocking sound.

3.6 Comparative Analysis Involving Widely Utilised Materials

A comparative analysis has been conducted to investigate the average transmission loss per unit thickness (dB/mm) of single-leaf structures based on the CJ samples. This analysis encompasses commonly utilised materials for noise reduction purposes[22]. The average TLs over a central frequency of seven 1/3-octave bands within 50-3150 Hz are graphically presented in Fig. 11. All the materials selected for comparison adhere to the principles of the mass law of sound[2,19].

Figure 11(a) illustrates that CJs provide the average transmission loss per unit thickness (dB/mm) for a given fibre content, displaying a consistent pattern. The observed trend suggests that the dB/mm value decreases as the thickness of the composite sample and the number of layers of jute nonwovens (N1, N2, N3) increase during the manufacturing of CJ. This leads to the conclusion that the relationship between TL and thickness is not linear. Therefore, for comparison with other commercial materials, thickness normalisation is necessary in the light of definition of transmission loss [Eq.(5)] and decibel[22]. The decibel (dB) is a logarithmic unit used to quantify the intensity of sound, representing the ratio between two values of power or root-power. Hence, the comparison study must involve thickness

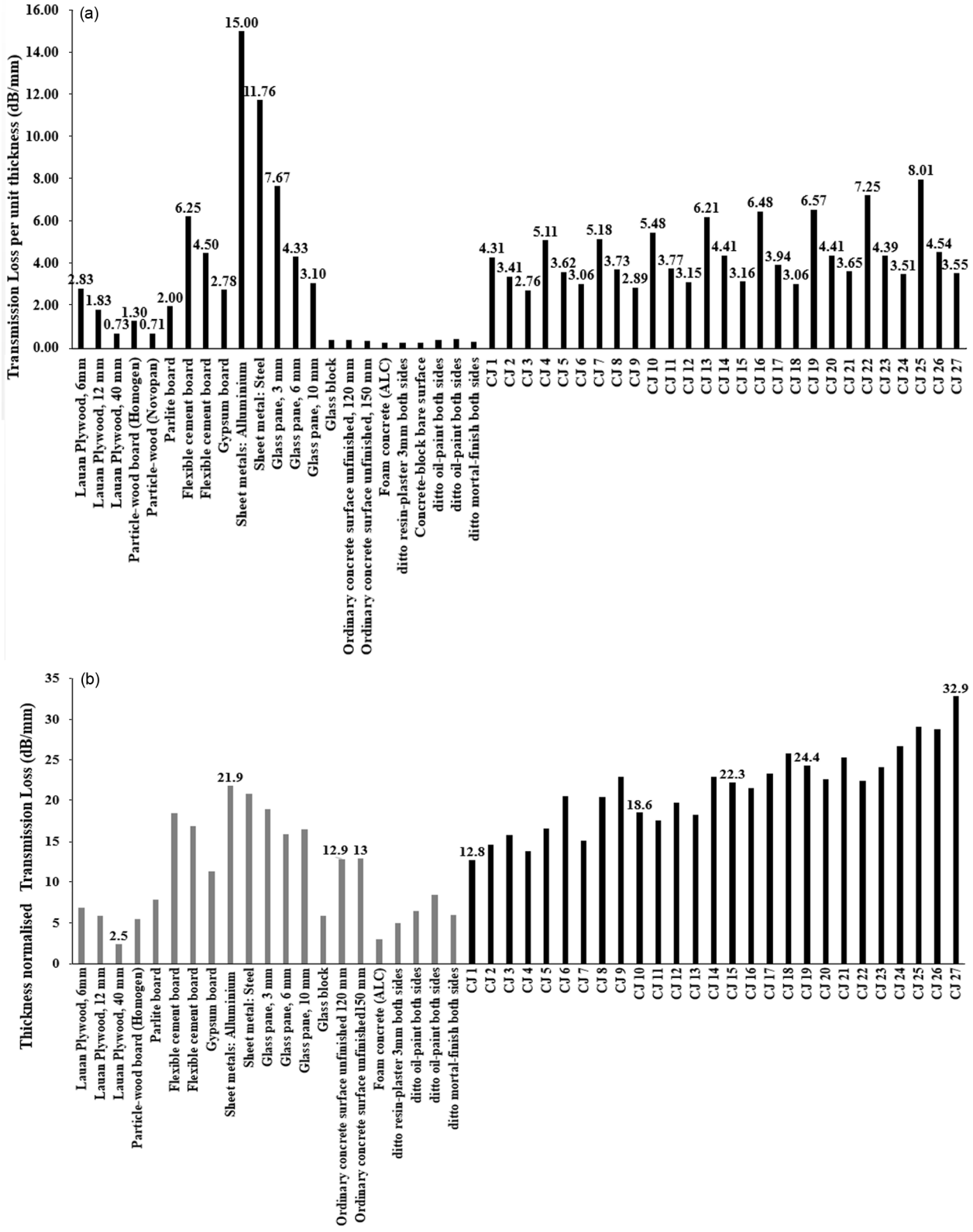

Fig. 11 — Plots of (a) average transmission loss/thickness and (b) thickness normalised average transmission loss of typical barrier materials along with all 27 samples

normalisation by subtracting log(thickness) from TL. The unit of thickness normalised TL (TL_{nor}) is also dB/mm, as the subtraction of log(thickness) represents the transmission loss/unit thickness.

Figure11(b) indicates a minimum TL_{nor} found in the case of the commercial grade Lauan plywood of 40 mm. The jute composite sample CJ1, with a thickness of 4.9 mm, exhibits the lowest normalised value of 12.8 dB/mm and that is found to be comparable to ordinary concrete of 120- and 150-mm thickness. In contrast, the largest value of 32.9 dB/mm is observed for the CJ27 sample, which has a thickness of 14.2 mm (Table 3). The thickness-normalised TL (TL_{nor}) increases with R_M following the trend like TL. Thickness normalisation of TL eliminates the effect of the number of layers of nonwoven (N1, N2, N3). It is found that for a given RM (3:1, 4:1, 5:1), with the increase of the areal density of reinforcing jute nonwoven (N1 <N2 <N3), TL_{nor} has an increasing trend. The performance exhibited by CJ 15 (22.3 dB/mm) is found comparable to that of 1.2 mm thick aluminium sheet metals which offers highest dB/mm of 21.9 among the widely used barrier materials.

4 Conclusion

The analysis of the physical properties of jute polyester composite materials shows that the existence of voids results in a decrease in the areal density of CJ at all the resin-to-material take-up ratios (R_M, which represents the amount of fibres present). A significant correlation is observed among the tensile, flexural, and impact strength of the composite samples (CJ) and the increase in bulk density. The elevated bulk density results in a reduced void content, thereby offering a more coherent and integrated structure for CJ.

The transmission loss (TL), exhibited by the single-leaf jute composite (CJ), conformed to the principles elucidated by the mass law of sound. The statistical analysis of the estimated transmission loss (TL) derived from Eq. (6), with a significance level of 1%, indicates that the generic model for the mass law of sound based on Cremer is needs to be adjusted. The analysis of experimental data of the transmission loss (TL) in jute composite materials suggested that the interaction between $\log_{10}(f)$ and $\log_{10}(m)$ were different. The regression equation, obtained through the least squares method, indicated that the coefficient for mass had higher magnitude compared to that of frequency in the range of 50-3150 Hz. The mass has thus more profound effect on transmission loss than frequency within this range. The transmission loss expression can be further deduced by considering the structural parameters, such as thickness and number of layers of jute nonwoven ($L = n \times t$), theoretical density (ρ_{th}), and the compaction factor (C_f). This allows for a straightforward prediction of sound transmission loss by engineering of the appropriate structural parameters (L_T,/L, ρ_{th}, C_f).

The literature review clearly highlights the challenging nature of designing an optimised single-leaf structure capable of effective reduction of sound level at lower frequencies. This study successfully engineered the single-leaf structures using jute composite, demonstrating significant transmission loss (TL), especially at a lower frequency of 50 Hz. The single-leaf structures based on jute composite (CJ) designed effectively, provide a transmission loss level comparable to or even higher than that of materials currently being utilised in practical applications. Therefore, it can be inferred that the engineered of single-leaf structure made of jute composite, provides a practical solution for mitigating noise issues for sustainable growth.

Acknowledgement

The authors are grateful to M/s Fibro Plastichem India Pvt. Ltd. for their support during the research.

References

1 King E A, *Environ Sci Policy Sustain Dev*, 64 (3) (2022) 17.
2 Janssen S, Van Belle L, de Melo Filho N G R, Desmet W, Claeys C & Deckers E, *Appl Acoust*, *213* (2023) 109622.
3 Mommertz E, *Acoustics and Sound Insulation: Principles, Planning, Examples* (De Gruyter, Munich, Germany), 2008.
4 Song S & Chen H, *Proceedings, Internoise17, Prediction of Sound Transmission Loss of Composite Floor Structures of High Speed Trains*, (Institute of Noise Control Engineering, Hong Kong, China), 2017, 33–38.
5 Zhang H, in *Building Materials in Civil Engineering,* by Zhang H (Woodhead Publishing, Cambridge Shire, United Kingdom),2010, 304–423.
6 Berardi U & Iannace G, *Build Environ*, 94 (2015) 840–852.
7 Mehrzad S, Taban E, Soltani P, Samaei S E & Khavanin A, *Build Environ*, 211 (2022) 108-753.
8 Sengupta S, Basu G, Datta M, Debnath S & Nath D, *J Text Inst*, 112 (1) (2021) 56–63.
9 Basu G, Datta M, Sengupta S, Nath D & Debnath S, *J Nat Fibers*, 19 (13) (2022) 6482–6496.
10 Tang X & Yan X, *Compos Part Appl Sci Manuf*, 101 (2017) 360–380.
11 Sur D, *Understanding Jute Yarn* (Anindita Sur, Kolkata, India), 2005.

12 Sheoran K, Siwal S S, Kapoor D, Singh N, Saini A K, Alsanie W F & Thakur V K, *ACS Eng Au*, *2* (5) (2022) 378.
13 Kuttruff H, *Room Acoustics* 4th edn. (Spon Press, London, England, New York, USA), 2000.
14 Mamtaz H, Fouladi M H, Al-Atabi M & Narayana Namasivayam S, *J Eng*, 2016 (2016).
15 Shen J, Li X & Yan X, *ACS Omega*, 6 (46) (2021) 31154.
16 Fatima S & Mohanty A R, *Appl Acoust*, 72 (2) (2011) 108.
17 Datta M, *Engineering of Jute Based Acoustic Insulator and Its Structural Analysis*, Ph.D. thesis, University of Calcutta, Kolkata, India, 2015.
18 Ng C F & Hui C K, *Appl Acoust*, 69 (4) (2008) 293.
19 Fahy F, in *Foundations of Engineering Acoustics* (Academic Press, London, England), 2000, 270–314.
20 Liu Z, *Design of Soundproof Panels via Metamaterial Concept*, Ph.D. thesis, School of Engineering Sciences, KTH Royal Institute of Technology, Stockholm, Sweden, 2019.
21 Rowell R, O'Dell J, Basak R K & Sarkar M, *Proceedings*, *Conference of National Institute of Research on Jute & Allied Fibre Technology* (NIRJAFT, Kolkata) 1997.
22 Maekawa Z, Rindel J & Lord P, *Environmental and Architectural Acoustics,* 2nd edn (CRC Press, London, England), 2010.
23 Sreekumar P A, Joseph K, Unnikrishnan G & Thomas S, *Compos Sci Technol*, 67 (3) (2007) 453.
24 Datta M, *India Pat*, 375300, 21 August 2015.
25 Hamidi Y K, Dharmavaram S, Aktas L & Altan M C, *J Eng Mater Technol*, 131 (2) (2009) 021-014.
26 Fardausy A, Kabir A M, Kabir H, Rahman M M, Ahmed K, Hossain F, Gafur A M & Begam A M, *Int J Adv Res Eng Tech*, 3 (2) (2012) 267.
27 Nath D, Debnath S, Datta M, Chakrabarti S, Ghosh S & Ghosh B, *J Ind Text*, 51 (7) (2022) 1121.
28 McMahon P E& Ying L, *Effects of Fiber/Matrix Interactions on the Properties of Graphite/Epoxy Composites.*(Celanese Corporation Summit NASA Contractor Report 3607, NewJersey, USA), 1982.
29 Rajak D K, Pagar D D, Menezes P L & Linul E, *Polymers*, 11 (10) (2019) 1667.
30 Yang X, Tang X, Ma L & Sun Y, *J Bioresour Bioprod*, 4 (2) (2019) 111.
31 Fang B, Theurich T, Krack M, Bergman L A & Vakakis A F, *Commun Nonlinear Sci Numer Simul*, 91 (2020) 105415.
32 Fan M & Fu F, in *Advanced High Strength Natural Fibre Composites in Construction*, (Woodhead Publishing, Cambridge shire, United Kingdom), 2016,1–20.
33 Guo H, Wang Y, Wang X & Xu C, *Adv Mech Eng*, 10 (1) (2018).
34 Rohatgi V K & Saleh A K M E, *An Introduction to Probability and Statistics* 2nd edn. (John Wiley & Amp Sons Inc, New York, USA), 2003.